Downloaded from SAE International by Columbia Univ, Wednesday, May 25, 2022

2022-01-0726 Published 29 Mar 2022

Electrical Insulation Properties of Alumina Coatings on SAE 52100 Bearing Steel

Dewei Deng, Ran Cai, Jiayi Sun, and Xueyuan Nie University of Windsor

Citation: Deng, D., Cai, R., Sun, J., and Nie, X., "Electrical Insulation Properties of Alumina Coatings on SAE 52100 Bearing Steel," SAE Technical Paper 2022-01-0726, 2022, doi:10.4271/2022-01-0726.

Received: 24 Jan 2022 Revised: 24 Jan 2022 Accepted: 11 Jan 2022

Abstract

In recent years, bearing electrical failures have been a significant concern in electric cars, restricting electric engine life. This work aims to introduce a coating approach for preventing electrical erosion on 52100 alloy steel samples, the most common material used on manufacturing bearings. This paper discusses the causes of shaft voltage and bearing currents, and summarizes standard electrical bearing failure mechanisms, such as morphological damages and lubrication failures. Alumina coatings are suitable for insulating the 52100 alloy steel samples because alumina coatings provide excellent insulation, hardness, and corrosion resistance, among other characteristics. The common method to coat an insulated alumina coating on the bearing is thermal spraying, but overspray can cause environmental issues, and the coating procedures are costly and time-consuming. Based on the research, this article briefly discusses employing plasma electrolytic aluminating to coat 52100 alloy steel samples, an eco-friendly and high-efficiency coating process. Coating experiments were conducted over different coating periods to determine the most appropriate thin film for 52100 alloy steel samples. Scanning electronic microscopy observations indicated that pores reduced as their size and porosity rose with the increased treatment time. Longer treatment period resulted in thicker coating layers, but a rougher surface. The results indicated that extending the coating period increased the insulating characteristics of the ceramic coating on 52100 alloy steel samples. The single piece of 20-minute coated sample had the best insulation property, compared with other single pieces. Two 20-min coatings sample combinations provided the best resistance (121–143 MΩ) and the highest breaking voltage (914–935 V). Coatings remained in good condition after thermal shock tests.

Introduction

Bearings play a crucial role in the electric engine because they connect the stationary and rotating parts of the motor and maintain the axis' rotation precision. Within an electric motor, bearings are the most sensitive and vulnerable components when the electric motor can vibrate and stop working because of the failure of the low-quality bearings, the automobile will lead to a significant car accident on the road.

The SAE 52100 bearing steel is unique steel with excellent wear resistance and rolling fatigue resistance, and it is commonly used in manufacturing bearings [1]. The shaft voltage is the potential difference between the motor's two bearing ends or between the motor shaft and the bearing. The alternating current (AC) asynchronous motor runs under the sinusoidal alternating magnetic field. When the electric motor's magnetic field is imbalanced, an alternating magnetic flux intersects with the motor shaft, inducing the shaft potential. A shaft current flows through the bearings on both sides of the shaft when a closed loop is formed [2]. Due to the low impedance of the current loop, a high shaft current is produced, which is highly damaging to the motor bearings [3]. During the operation of the electric engine, the overcurrent can damage the surface of bearing raceways, rolling bearing components and cause lubricants to age prematurely, resulting in motor or generator failure [4].

Under normal conditions, a lubricating oil coating forms on the shaft and bearing as an insulation layer. For lower shaft voltages, the lubricating film still can protect bearing from electrical damages. However, when the shaft voltage reaches a certain level instantly and the oil film does not form a stable film, the shaft voltage breaks down the oil film and discharges. Due to limited contact area, the current density is high, making the instant high temperature in bearings. Simultaneously, the motor bearing temperature rises fast, accompanied by lubricating grease evaporation [5]. The bearings are partially melted, and the melted alloy spills on the inner surface, forming the pits. Generally, the inner surface of the bearing is usually pressed out with spark traces because the spinning shaft's hardness and mechanical strength are higher than the molten alloy of the bearing. The fluting of the raceways is the second typical damage caused by the

Downloaded from SAE International by Columbia Univ, Wednesday, May 25, 2022

transmission of harmful electrical current through the bearing [6].

The ceramic layer formed on the aluminium alloy's plasma arc treatment on the surface is mainly made up of crystalline Al_2O_3. The high resistance of α-Al_2O_3 and γ-Al_2O_3 determines the high insulation of the plasma electrolytic oxidation ceramic layer. The high number of γ-Al_2O_3 results in high insulation [7].

Using insulated bearings at the motor design stage is a more cost-effective approach, significantly lowering the equipment's maintenance costs and increasing the machine's usage rate. The production of insulated bearings is usually applied to a highly insulating ceramic coating on the external surface of the inner bore (ID) or outside ring (OD) by thermal spraying. Currently, most insulating bearings are coated on one side. It is important to investigate whether double coating improves insulation, so two coatings overlapping combination, like a "sandwich" shape, should be used for simulating when alumina films are applied on the inner bore and outside surface of the bearing [6]. During thermal spraying, oxide particles are melted by a hot plasma stream. In the pre-treated substrate, the molten particles cool down and form the required coating on the substrate. The insulating coating is a lamellar structure composed of deformed molten particles and powder particles. The pores and metastable phases in the coatings can reduce the insulation performance of the coatings. Rajaram et al. [8] stated that sealing the alumina coating was needed to improve its insulating properties by preventing conduction between the interior and outside of the coating. Even though the bond coat can improve the bonding strength, hardness and lower the porosity, the insulation property became weaker than the only alumina coated samples. The heated materials and coating overspray can produce some fumes and dust. Therefore, obtaining the alumina coating by thermal spraying needs more coating procedures, and the coating methods are also time-consuming and costly.

Plasma electrolytic aluminating (PEA) is a repeatable process that generates the hercynite–alumina composite coating on the surface of metal objects in room temperature by using high voltage and current. Besides, no hazardous gas is produced during processing, and residual liquid discharge can meet environmental protection requirements [9]. In stage 1 of PEA process, the Al $(OH)_4^-$ ions are spread uniformly throughout the electrolyte before applying current. Stage 2, anode loses the electron in the oxides, and iron dissolves into the Fe^{2+} ions. Stage 3, gas is discharged from the oxide hole, resulting in melting the surface material. Al $(OH)_4^-$ ions interact with Fe^{2+} ions on the anode surface to create an iron spinel ($FeAl_2O_4$) layer. When a continuous layer of Fe-Al spinel fully covers the surface, the plasma is produced. Thermal diffusion forms the deposition of colloidal particles. The negatively charged colloidal particles migrate into the discharge channel. Al $(OH)_4^-$ ions move to the anode and adsorb on the spinel layer. In the elevated temperature of plasma, the Al $(OH)_4^-$ ion is converted to Al_2O_3 and subsequently sintered with $FeAl_2O_4$ [10]. Furthermore, throughout the process, oxygen is emitted as bubbles. Stage 4, an intense plasma discharge may melt iron in the substrates and spray it to the surface along the discharge channel because the plasma discharge interacts with thermochemistry. This molten iron may serve as a supply of iron for the formation of the iron spinel alumina composite ceramic covering. Under the ambient temperature coating condition, a thick functional ceramic coating is generated on the steel alloy's surface by micro-arc discharge in the electrolyte with a high voltage and large current. The coating is highly durable and resistant to corrosion. Simultaneously, it exhibits great properties of electrical insulation.

This paper introduces a new, low-cost, high efficiency and environmentally friendly method to coat the general bearing steel materials. Using the PEA coating method can overcome the drawbacks of low-binding strength and enhance the insulation performance of alumina coatings on the substrates. In the primary research stage, the plasma electrolytic aluminating coating was applied on bearing steel pieces. This article performs scanning electronic microscopy (SEM) analysis on the coated test samples to investigate the effect of experiment time on the change of ceramic layers. The surface profiler was used to obtain the average surface roughness Ra, and the reduced peak height, Rpk. The insulation property was determined by the measured value of breaking voltage and electrical resistivity, followed by the coating process. To determine the coating's thermal stability, 50 times thermal shock tests were done on the coating which had best insulation properties

Experimental Section

Using the plasma electrolytic aluminating (PEA) technique, the bearing steel samples were ceramic coated in this experiment. Each sample was 25.4 mm in diameter and 5.00 mm thick.

In the experimental preparation stage, five precoated samples were cut out of bearing steel SAE 52100 rod. The chemical compositions of the bearing steel were Fe (96.5-97.3%), Cr (1.3-1.6%), C (0.9-1.1), Mn (0.25-0.45%), Si (0.15-0.3%), S (≤0.025%) and P (≤0.025) [1]. Before the coating process, the specimens were ground slightly on SiC papers with reduced particle size by hand to remove the oxide layer or dirt on the surface.

FIGURE 1 Illustration of the structure of the vital PEA experimental apparatuses.

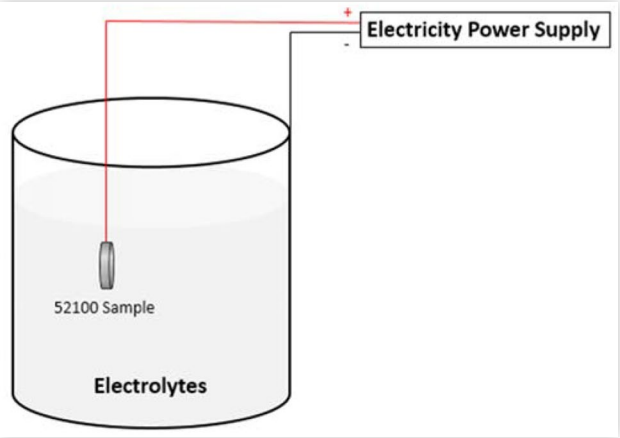

Downloaded from SAE International by Columbia Univ, Wednesday, May 25, 2022

Figure 1 shows the PEA experimental equipment. Step 1 of the experiment procedures, the passivation treatment was applied on each sample quickly by PEA coating. The purpose of a passivation treatment was to form a protective film on a cleaned metal surface to slow corrosion. Step 2, the entire sample was immersed in the electrolyte solution, containing 15-20g/L $NaAlO_2$ and 3-5g/L Na_3PO_4, after the completed passivation procedure. Step 3, a constant power supply index of voltage 510V, frequency 1 kHz was used for the specified period for the coating procedure. Step 4, the coated sample was slightly polished with high grid SiC sandpaper after PEA treatment. The experiment was designed into five groups based on the different treatment periods, 5 mins, 10 mins, 15 mins, 20 mins, and 20 mins with same conditions.

After the coating experiment, the scanning electronic microscopy (SEM) was used to examine the surface and cross-section microstructures after the coating test. The coated pieces were slightly polished before the SEM analysis. After grinding and polishing, the cross-section of one half of a coated sample was studied under the SEM to determine the thickness of the alumina coatings, and energy dispersive spectroscopy (EDS) revealed the cross-element section's distribution. Repeated the steps for all coated samples.

Roughness values of the samples were measured by a Mitutoyo SJ-201 surface profiler. Measurements of each sample were repeated five times, and the average surface roughness Ra and the reduced peak height, Rpk were obtained.

Before the measurement procedure, the one sides of the samples were removed by sandpapers to meet the requirement of measurement procedure of the megohmmeter. FLUKE 1550B megohmmeter, which measured up to 1 Tera-Ohm, was used to measure the insulation resistance of the samples. The measurement condition was 265V DC, and the measurement period was 10 min for each sample under pressure gauge. After the resistivity tests, the breaking voltage tests were applied. Each test was repeated five times and the average values were obtained. The best results of two sample combinations of two coatings overlapping in a sandwich shape were measured at the end of this test to simulate the state of PEA coating on both inner bore and outside rings of the bearings.

The coated sample was heated for 15 minutes at 500 degrees Celsius in the furnace. The sample should be cooled in room temperature water. After that, the sample was dried by air. It was necessary to investigate the coatings whether was peeled off after each thermal shock test. Repeat the experiment steps 50 times. SEM observation should be applied to determine whether thermal shock tests impacted the surface microstructures of the coatings.

Results and Discussion

Scanning Electronic Microscopy (SEM) Analysis

Figure 2 indicates SEM observation of the stereoscopic morphology of the samples.

Based on surface SEM images, the surface morphology mainly consists of cooled oxides, discharge holes, and cracks.

FIGURE 2 SEM images (x600) of the coating surfaces of different PEA treatment periods, (a) 5 mins PEA treatment, (b) 20 mins PEA treatment.

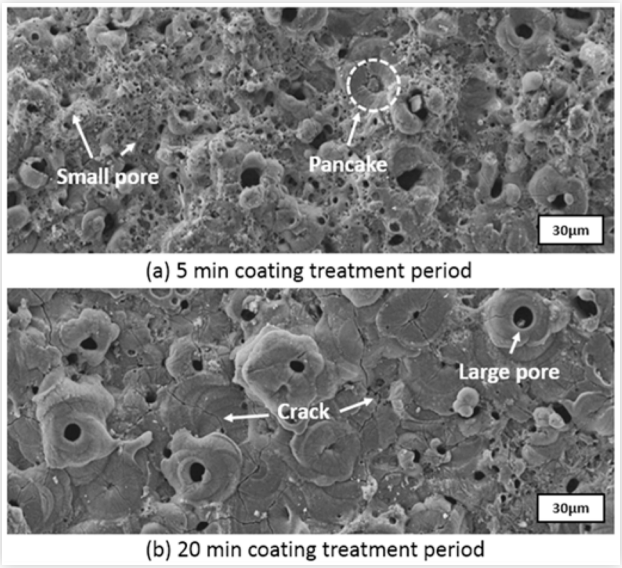

On the surface of the hercynite–alumina composite layer, several "donut" shapes of the molten pools are linked to one another. Due to the rapid reaction, fast cooling, and solidification of molten oxide, the formation of this structure was produced during the plasma discharge process in the electrolyte solution [11]. The dimensions of discharged pores are 3-10 μm in diameter.

The sample's surface can be coated with a ceramic layer after plasma electrolytic aluminating. Based on Figure 2, the number of surface holes on alumina layers are gradually reduced, but the size of the hole area gradually become larger with the increasing PEA treatment time. The film's surface was porous with many disordered holes resembling "craters" created from micro-arc discharges. There was a significant quantity of condensed $FeAl_2O_4{\cdot}Al_2O_3$ surrounding these pores, like "pancake" shapes, increasing the thickness of the substrates with a longer duration [12]. The SEM figures show that the alumina film created by plasma electrolytic aluminating technology is formed on the metal surface by metallurgical bonding, resulting in a solid connection. The number of small pores reduced as the length of PEA therapy increased. The small pores were broken apart and absorbed into the molten products with the increasing PEA treatment period. The fewest small pores are showed in the SEM figure of the 20-minute PEA treatment. When the PEA treatment time was extended, fewer cracks and micropores appeared on the alumina coating surfaces. During plasma discharges, "crack" and pores, resulted from high-pressure gases escaped from the molten zone. The number of surface holes was reduced, but the size of the hole area became larger with the increasing PEA treatment time. As a result, there were fewer holes and cracks, resulting in a stronger binding strength of the alumina coatings and the alumina coatings became more durable.

The alumina coating's cross-sectional morphology under SEM observation indicates the coating's thickness in Figure 3. The coating's performance is determined by its characteristics

Downloaded from SAE International by Columbia Univ, Wednesday, May 25, 2022

FIGURE 3 The SEM images (x800) of the cross-sections of different PEA treatment periods, (a)5 mins PEA treatment, (b) 20 mins PEA treatment.

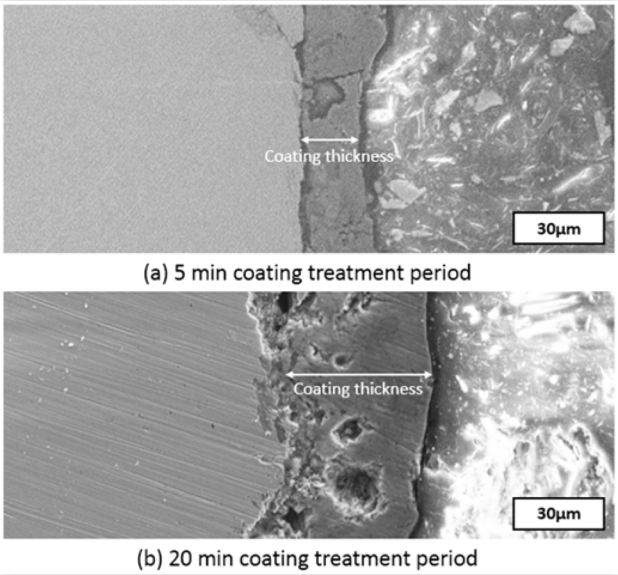

and the bonding strength between the coating and the substrate.

The cross-sectional morphology of the composite coating reveals that there are three layers from the left-hand side to the right-hand side, a bearing steel samples' layer, the hercynite–alumina composite layer, and an acrylic resin layer.

The film's section morphology mainly reflects the film's local thickness and adhesion to the bearing steel samples. The film's performance is determined by its characteristics, and the film's bonding strength with the test samples [13].

As shown from the enlarged Figure 3, the oxide melts in the plasma discharged region cover the existing pores and other weak parts of the examined sample by forming alumina layers so that the PEA technique can create a dense protective coating. As a result, the alumina coating formed on the surface of the tested sample was able to enhance the metallic properties of the substrates. The "craters" were formed because of micro-arc oxidation. Due to the rapid reaction and fast cooling, some vents of the "craters" were not entirely closed, and another layer is applied to them quickly without solidifying melts [14]. The continuous uniform discharge of plasma on the steel sample resulted in the fusion and connection of these craters, forming the reason for the transverse holes in the cross-section.

From Figure 3, the lowest thickness of the alumina coating is about 20 μm with the 5-min coating treatment period, and the highest thickness of the alumina coating is found during the 20-min coating treating period, which is about 35 μm.

By comparisons and research reviews, as the experiment period goes on, the thickness of the alumina ceramic film grows thicker, and the density of the alumina ceramic film increases as well.

FIGURE 4 EDS mapping analysis of the chemical composition of the cross-section of alumina layer for different coated samples.

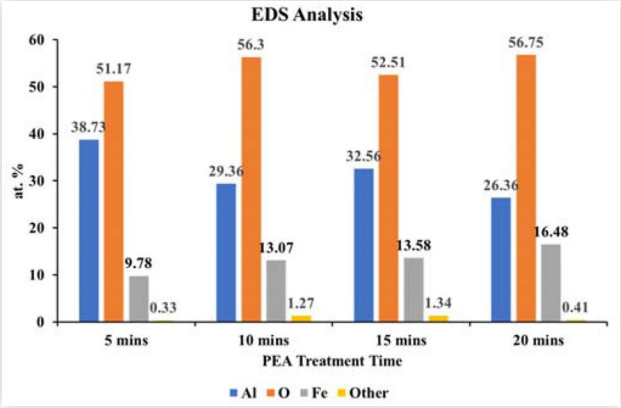

Energy Dispersive Spectroscopy (EDS) Analysis

EDS analysis was used to study the general element' chemical composition of the cross-sections of ceramic coatings. Chemical compositions of the alumina coating on tested samples are summarized in the column diagram shown in Figure 4.

Al element contents in the cross-section layers were relatively high in coated samples, and it gradually decreased with the increasing treatment duration and an increasing amount of iron to participate in the reaction with the rose in Fe element contents. The lowest percentage of the ferrous element occurred in the 5 min coated sample and the highest percentage of the ferrous element was observed in the 20 min coated sample. According to the behavior of electrochemical reaction [15], when a deposition reaction occurred during the micro-arc oxidation process on the substrate's surface, alumina layers' formation happened more frequently in the certain short period, more alumina deposited on the metal's surface. Other ions in the electrolyte were deposited and adsorbed to the ceramic film by the electrochemical process on the outer layer. Based on the cross-section figures, the increasing thickness of hercynite–alumina composite coating causes the growing amount of Fe element on the surface by forming more $FeAl_2O_4{\cdot}Al_2O_3$ components on the substrate.

Roughness

The roughness results were obtained by using the Mitutoyo SJ-201, as indicated in Figure 5.

Ra, the average roughness value, was tested with a starting value of 2.966 μm that was measured five minutes after the test started, and it showed a steady increase to 3.364 μm within the first ten minutes. Then, within the next five minutes, it dropped sharply to 1.742 μm. It showed a quick increase to a high value of 3.916 μm at twenty minutes after reaching the lowest roughness during the testing period. The testing results of Rpk, highest profile peak height, followed the same pattern

Downloaded from SAE International by Columbia Univ, Wednesday, May 25, 2022

FIGURE 5 The roughness results from different coating periods.

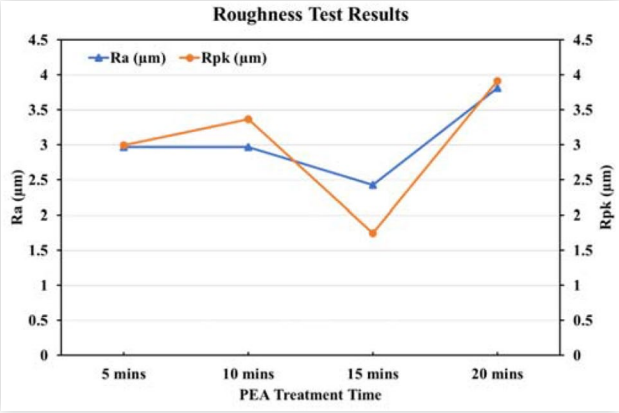

FIGURE 6 The layer application demonstration diagram with increasing treatment periods, (a)5 mins PEA treatment on sample 1, (b) 10 mins PEA treatment on sample 2, (c) 15 mins PEA treatment on sample 3, (d) 20 mins PEA treatment on sample 4.

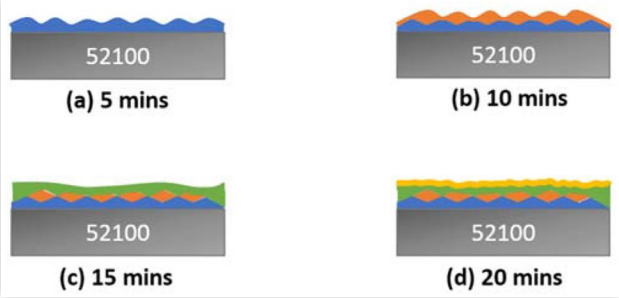

as Ra's, slightly decreasing from 2.992 μm to 2.968 μm for the first five minutes. Following that, a mild fell to 2.424 at fifteen minutes and a rose to 3.814 at twenty minutes.

According to the demonstration diagram of layer application shown in Figure 6, different colors of the layers represent the sequence of the alumina layer application, which impacts the level of flatness of the surfaces. The fluctuation of the roughness value is that the more extended period of PEA treatment will fulfil the pores of the surface of alumina coating by applying one layer on top of another layer. The surface roughness with the increasing PEA processing time rose as the increasing diameters of craters and the pancake's height.

The pore at the grain boundary was the primary factor for the difference in hercynite–alumina composite layers' surface roughness. The tiny grain structure facilitated the distribution of pores uniformly, decreased the direct longitude of holes, and reduced surface roughness [11]. Lower roughness values contribute to a smoother surface. Compared to the rough surface, the smooth surface can improve the wear resistance. The coating quality, thermal conductivity, and electrical resistance are all influenced by surface roughness to variable degrees [16]. Therefore, it is necessary to control the roughness value after the coating procedure.

Breaking Voltage and Resistivity

The hercynite-alumina coating on steel alloy substrate with good insulation properties should have the higher breaking voltage and resistance. Figure 7 shows the average breaking voltage and average resistivity with different coating duration.

The experimental results revealed that the thickness of the ceramic oxide coating grew with the increasing treatment time, reaching its maximum thickness at 20 minutes when no yellow plasma sparks occurred on the substrate. The quantity of plasma electrolytic deposited on the metal surface rises as the reaction time increases. In the insulation test results, the average breaking voltage showed a stable increase for 15 minutes, followed by a steep rise later. In comparison, the average resistivity showed steady growth for the whole testing result. Comparing the 5-minute PEA treatment duration with 20-min PEA treatment duration of single piece sample, the average value of breaking voltage was almost double, from 414.29 V to 764.67 V. The lowest average resistivity was 13.6 MΩ, and the highest average resistivity was 93.65 MΩ. The resistivity of the coated samples increased tenfold from the low period treatment to the long period treatment. The increasing coating treatment period can improve the insulation properties of the coatings on the bearing steel samples. According to the test design, two 20-minute coated sample combinations should be used for imitating when alumina films were applied on the inner bore and outside surface of the bearing. The electric resistance and breaking voltage of 20-minute treatment samples combinations with two coatings overlapping with a "sandwich" shape were much higher than those of a single coated sample. The breaking voltage of the combinations was 914-935 V, and the resistivity of the combinations was 121-143 MΩ. As can be observed, if the bearing can be coated on both sides with alumina, the insulation capability will be increased.

The ratio of the resistivity efficiency is the amount of resistance divided by the thickness of coatings. Compared to the research project done by Rajaram et al. [8], the resistivity efficiency of the thermal spraying coating with bond coat was

FIGURE 7 The average breaking voltage and average resistivity with different coating duration.

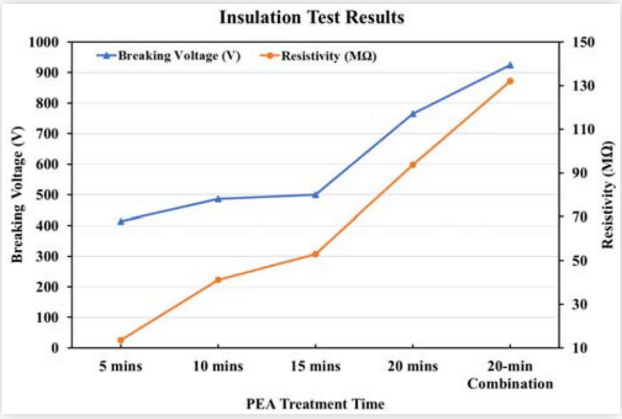

Downloaded from SAE International by Columbia Univ, Wednesday, May 25, 2022

FIGURE 8 The scanning electronic microscopy (SEM) surface images of 20-min coated sample before heating (a) and 500 °C heated (b).

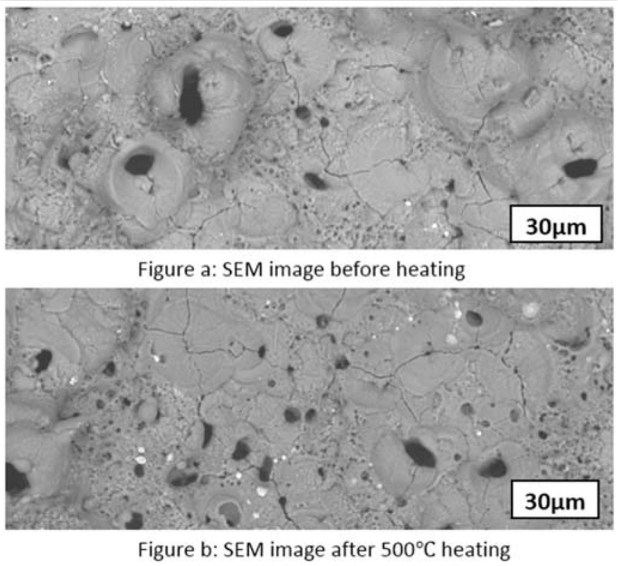

about 10 MΩ/μm. As for the resistivity efficiency of the plasma electrolyte aluminating coated sample was roughly 22 MΩ/μm. As a result, the same thickness of alumina coating produced by PEA coating has the larger electrical resistivity. The insulation performance of the PEA coated sample is stronger than the sample coated by thermal spraying with the bond coated.

Thermal Shock Tests

Thermal shock tests are determined the stability of the microstructures of the coatings under 500 °C heated by furnace and rapid cooled down by room temperature water. SEM images in Figure 8 shows the change of the microstructure of the thickest coating after thermal shock tests.

The cracks on the alumina coating became deepen and more visible under backscattered electron imaging (BEI) mode of SEM at the high magnification. Meanwhile, an increasing amount of micropores appeared on 500 °C heated coatings. The number of pores on the surface of coated sample was increased compared to the surface image of the non-heat-treated coated sample. The size of cavity increased, and more large cavities might also be seen on the surface. However, the coating was not peeled off from the steel alloy substrate after 50-time thermal shock tests.

Conclusion

Hercynite-alumina composite coating was successfully produced on the steel alloy 52100 substrates by using the plasma electrolytic aluminating method with different treatment durations (5, 10, 15, and 20 minutes). It was found that the alumina coatings' insulation properties were influenced by the different surface morphologies and number of discharge holes. The thickest coating had the strongest insulation performance and the deposition rate on the substrate was 1.75 μm/min. Coatings maintain good condition after thermal shock tests. In general, if the long period of plasma electrolytic aluminating coating is applied, it will be recommended to lightly polish to reduce roughness to retain the bearing's service performance. Double alumina layers with the maximum coating treatment periods should be applied on the inner bore (ID) and outside surface (OD) of bearings to enhance the insulation performance. Compared to the advanced thermal spraying method, using plasma electrolytic aluminating method can avoid thermal or heat distortion effects potentially from coating processing. However, the insulation performance of the alumina coatings on the real bearing applied by plasma electrolytic aluminating treatment must be investigated at the next research level. The plasma electrolytic aluminating coating duration is not the only factor influencing the quality of alumina coating since it is a complicated process. The quality of the oxide ceramic film is influenced by many technical factors, such as the different electrolyte's chemical compositions, various bearing (anodic) materials, different voltages, and currents to be applied. Further studies are required to discover the optimum insulation performance of alumina coating on real bearings.

References

1. Pan, Y., Wang, B., and Barber, G.C., "Study of Bainitic Transformation Kinetics in SAE 52100 steel," *Journal of Materials Research and Technology* 8, no. 5 (2019): 4569-4576, doi:10.1016/j.jmrt.2019.08.001.
2. Kolic, E., "Bearing Current and Shaft Voltage Measurement in Electrical Motors," Bachelor's Thesis, Department of Engineering Science, University West, 2017.
3. Baldor, "Part 2-Shaft Voltage and Bearing Current," https://www.motionindustries.com/, accessed on Sep. 2021.
4. He, F., Xie, G., and Luo, J., "Electrical Bearing Failures in Electric Vehicles," *Friction* 8, no. 1 (2020): 4-28, doi:10.1007/s40544-019-0356-5.
5. Booser, E.R. and Khonsari, M.M., "Grease Life in Ball Bearings: The Effect of Temperatures," *Tribology and Lubrication Technology* 66, no. 10 (2010): 36-38, 40-42, 44.
6. SKF, *Bearing Damage and Failure Analysis* (SKF Group, Pub BU/I3 14219/2 EN, 2017)
7. Gao, J., Xiong, X., and Gao, Y., "The Effect of the α/γ Phase on the Dielectric Properties of Plasma Sprayed Al_2O_3 Coatings," *Journal of Materials Science: Materials in Electronics* 28, no. 7 (2017).
8. Rajaram, G. and Jain, A., "Characteristics of Alumina Coating on SAE 52100 Bearing Steel with Ni-Cr Bond Coat," *International Journal of Materials Engineering Innovation* 9, no. 20 (2018), doi:10.1504/IJMATEI.2018.092183.
9. Zhao, C., Zha, W., Cai, R., Nie, X. et al., "A New Eco-friendly Anticorrosion Strategy for Ferrous Metals: Plasma Electrolytic Aluminating," *ACS Sustainable Chemistry &*

Downloaded from SAE International by Columbia Univ, Wednesday, May 25, 2022

Engineering 7, no. 5 (2019): 5524-5531, doi:10.1021/acssuschemeng.8b06839.

10. Hussein, R.O., Nie, X., Northwood, D.O., Yerokhin, A. et al., "A Spectroscopic Study of Electrolytic Plasma and Discharging Behaviour During the Plasma Electrolytic Oxidation (PEO) Process," *J. Phys. D: Appl. Phys.* 43 (2010): 105203-105216.
11. Erfanifar, E., Aliofkhazraei, M., Fakhr Nabavi, H., Sharifi, H. et al., "Growth Kinetics and Morphology of Plasma Electrolytic Oxidation Coating on Aluminum," *Materials Chemistry and Physics* 185 (2017): 162-175, doi:10.1016/j.matchemphys.2016.10.019.
12. Tillmann, W., Khalil, O., and Abdulgader, M., "Porosity Characterization and its Effect on Thermal Properties of APS-Sprayed Alumina Coatings," *Coatings* 9, no. 10: 601, doi:10.3390/coatings9100601.
13. Abrahami, S.T., De Kok, J.M.M., Gudla, V.C., Ambat, R. et al., "Interface Strength and Degradation of Adhesively Bonded Porous Aluminum Oxides," *Npj Materials Degradation* 1, no. 1 (2017), doi:10.1038/s41529-017-0007-0.
14. Amsellem, O., Borit, F., Guipont, V., Jeandin, M., and Pauchet, F., "A Composite Approach to Al_2O_3 Based Plasma-Sprayed Coatings." in *Presented at the 20th International Conference on Surface Modification Technologies*, Vienne, Austria, Sep 2006, 2017.
15. Simchen, F., Sieber, M., Kopp, A., and Lampke, T., "Introduction to Plasma Electrolytic Oxidation—An Overview of the Process and Applications," *Coatings* 10, no. 7 (2020): 628, doi:10.3390/coatings10070628.
16. Arabgol, Z., Villa Vidallerb, M., Assadi, H., Gärtner, F. et al., "Influence of Thermal Properties and Temperature of Substrate on the Quality of Cold-Sprayed Deposits," *Acta Materialia* 127 (2017), doi:10.1016/j.actamat.2017.01.040.

Contact Information

Xueyuan Nie, Ph.D., Professor,
Mechanical, Automotive & Materials Engineering,
University of Windsor,
401 Sunset Avenue,
Windsor,
Ontario, N9B 3P4,
Canada,
+1 519-253-3000, ext. 4148,
xnie@uwindsor.ca

Acknowledgments

This research was supported by Natural Sciences and Engineering Research Council of Canada (NSERC).

Definitions/Abbreviations

SEM - scanning electron microscope

AC - alternating current

PEA - plasma electrolytic aluminating

EDS - energy dispersive spectroscopy

BEI - backscattered electron imaging

SEI - secondary electron imaging

ID - inside diameter

OD - outside diameter

© 2022 SAE International. All rights reserved. No part of this publication may be reproduced, stored in a retrieval system, or transmitted, in any form or by any means, electronic, mechanical, photocopying, recording, or otherwise, without the prior written permission of SAE International.

Positions and opinions advanced in this work are those of the author(s) and not necessarily those of SAE International. Responsibility for the content of the work lies solely with the author(s).

ISSN 0148-7191